LTE-based Wireless Channel Modeling on High-Speed Railway at 465MHz

Yanfei Niu*, Jianwen Ding⋆†, Dan Fei*†, Zhangdui Zhong*†, Yanbing Liu‡
*State Key Laboratory of Rail Traffic Control and Safety, Beijing Jiaotong University, China
⋆National Research Center of Railway Safety Assessment, Beijing Jiaotong University, China
†Beijing Engineering Research Center of High-speed Railway Broadband Mobile Communications, China
‡Mobile and Broadband Internet Technology Research Institute, Jiaxun Feihong Intelligent Technology Institute, China
Jianwen Ding (Corresponding Author) Email: jwding@bjtu.edu.cn

***Abstract*—A practical and novel research of radio propagation channel modeling is mainly presented in this paper. This is the first comprehensive result of path loss, large-scale fading and small-scale fading under long-term evolution frequency division duplex railway testing network (LTE-R) whose downlink center frequency is set at 465MHz, bandwidth is 5MHz. Besides, a detailed description of the measurement system as well as the measurement scenario is introduced. Our measurement campaigns were carried out under multiple-input multiple-output with top train speed of 340km/h. Based on the measurement data, the empirical path loss model is studied. Probability density functions of large-scale fading and small-scale fading are discussed. Channel characteristics such as path loss attenuation exponent, standard deviation of shadowing and Rician K-factor are shown. The statistical channel models are established to characterize the high-speed railway (HSR) scenarios which can contribute to evaluating and significantly promoting the network performance.**

***Index Terms*—LTE-R, measurement, channel modeling, characteristic, HSR**

I. Introduction

Recent years, high-speed railway (HSR) has made great strides in China. Global system for mobile communications for railway (GSM-R) that adopts frequency of 900 MHz is used to transmit train-controlling information in China now. Only voice and a small amount of data service can be transmitted by GSM-R system. With the diversified demands of railway service and the increase of train speed, the GSM-R system can no longer support the development of the railway[1]. Therefore, it is extremely urgent to change the wireless access system to make up for the disadvantages.

Long-term evolution for railway (LTE-R) is deemed to be the next generation communication system to support the growth of railway service. The first LTE-R testing network was deployed in 2018. At present, LTE-R wireless channel research is underway. Numerous HSR channel researches are shown. For example, Goller conducted channel testing of the GSM-R system in the German HSR with center frequency of 945MHz and train speed of 250km/h in 1995. Measurement scenarios included rural, urban and mountain areas. The results of Rician parameter, fading depth, and delay extension were obtained. It is the first time to conduct wireless channel parameter analysis through testing[2]. The test was conducted in the 1990s. So the results no longer can apply to the study of LTE-R network with a top speed of 340km/h. A research based on the HSR viaduct scenario at 2.35GHz with 240km/h is proposed in[3]. It established a channel model about path loss and analyzes the propagation mechanisms with a geographical perspective. There also has been described statistical analysis of radio wave propagation in a HSR cutting scenario, derived from 930MHz measurements[4]. Reference [5] presents the results of path loss measurements in different HSR environment at 930Mhz. Even if reference [3]-[5] on the wireless channel models are comprehensive, it does not conform to the LTE-R network as mentioned. The channel model of LTE-R is quite different from the channel model of public LTE cellular network. Both geographical environment and channel parameters setting have a very large influence on wireless communication. Measurement methods for studing the radio propagation models are adopted by us to fill the blank of wireless channel research. An empirical path loss model, the analysis of large-scale fading and small-scale fading of broadband LTE-R network is performed in this paper, together with fading distribution fitting. This paper can provide a theoretical basis for future LTE-R study and application in the HSR.

The structure of this paper is organized as follows: In section II, the measurement scenario and measurement system are introduced in detail. The path loss, large-scale fading and small-scale fading model are presented in section III. This part discusses attenuation exponent n_{att}, standard deviation of shadowing and Rician K-factor as well. Section IV concludes the paper.

II. Measurement Campaign

A. Measurement Scenario

The scenario of our measurement campaign in this paper is typical rural area as shown in Fig. 1. The distance from the beginning to the end is about 3km. Most of the buildings within the effective coverage are low-rise houses. And some

The authors express their thanks to the support in part from the National Key R&D Program of China under Grant No.2018YFB1201500 and No.2016YFE0200900, the Project of China Railway Corporation under Grant (N2018G025, N2018G072 and P2018G052), and the Research Funding of ZTE.

978-9-0827-9703-9/19/$31.00 ©2019 IEEE

Fig. 1. Measurement scenario.

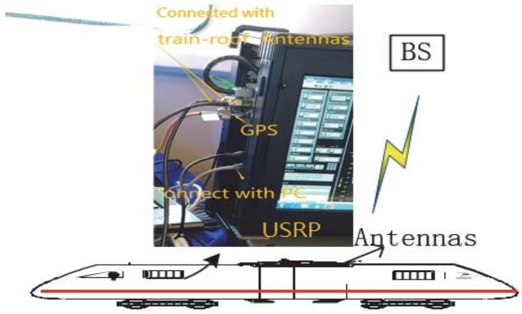

Fig. 2. Measurement system.

trees are in height of 3m to 8m. Weather conditions during the measurement campaign are range from sunny to cloudy.

The distance between base station (BS) indexed to green in Fig. 1 and railroad is 18m. The frequency of the adjacent BS is the same, which is 465MHz. Two cross-polarization directional LTE-R antennas about 40m height with an azimuth angle of $45°$ or $225°$ are fixed on the BS. The downward inclination angle of antennas is $4°$. The measurement start point is marked to red and the yellow line is measurement route.

B. Measurement System

The physical channel measurement about LTE-R network is implemented based on universal software radio peripheral (USRP). The USRP has two ports for receiving and transmitting data. Two omnidirectional antennas connected with USRP are mounted on the train roof, providing a total antenna height of 4.05m above the railroad. A large penetration loss approximately 20dB caused by the train body can be avoided by this method. Global Positioning System (GPS) receiver is equipped in the USRP to obtain the consistent time, train speed and location information. Meanwhile, the USRP can be used for data processing, analysis and storage in real time. Finally, measurement system is shown as Fig. 2. The received measurement data by equal time interval sampling which related to LTE-R system bandwidth are completely stored on a solid state disk as I/Q data. The stored measurement data contains all the information of the wireless channel. The measurement parameter setting is presented in Table I.

TABLE I
MEASUREMENT PARAMETERS

Parameters	***Setting***
Transmission Mode	LTE FDD
Center frequency, f	465MHz
Transmit Power, P_{Tx}	43dBm
Bandwidth, BW	5MHz
Tx antenna gain	12dBi
Rx antenna gain	4dBi
Sample rate, f_s	7.68MHz
Delay resolution, $\Delta\tau$=1/BW	0.2μs
Snapshot repetition period, t_{rep}	0.25ms

With these settings, the theoretical maximum Doppler shift is about 146Hz with the maximum speed of 340km/h. Synchronization, cell search, demodulation, and resource mapping are carried out in order to extract the cell-specific reference signal (CRS) from the I/Q data[6]. One of the four subchannel is analyzed to obtain channel model. Reference signal receiving power (RSRP) can be obtained from the received CRS. The ratio of the received CRS to transmitted CRS is the channel frequency response (CFR). At last, complex channel impulse response (CIR) can be recovered by calculating an inverse fourier transform (IFFT) of CFR, using the Hanning window. In our analysis, CIR stored in an array of size $N * K * P$ are collected, expressed as $h(nt_{rep}, k\Delta\tau, p)$. Here, N = 43120, K = 50, P = 4, n is the time index with $n = 1, 2, \ldots, 43120$, k is the delay index with $k = 1, 2, \ldots, 50$, and p is the channel number with $p = 1, 2, \ldots, 4$.

III. EVALUATION RESULTS

A. Path Loss

Path loss (PL) is used to show the signal attenuation as a positive quantity measured in dB which is caused by the dissipation of the power radiated by the transmitter as well as effects of the propagation channel. Before performing the model estimation, measured data needs to be pre-processed to keep the data effective[7]. The pre-processing includes: smooth the data, remove the near-field data and correct the GPS error. The received signal power ($\overline{P_{Rx}}$) should be calculated first to get PL. In general, the RSRP values can be utilized to indicate the received signal power in LTE-R network. In this paper, a RSRP value is got from the average of one frame of a subchannel which contains 40 CRS. The distance between two adjacent RSRP values is about 1.9m. All RSRP data after pre-processing cover distance over 1km.

The transmit signal power (P_{Tx}) is about 43dBm. The PL can be got by taking the difference value between transmit signal power and received signal power, which can be denoted by

$$\overline{PL}(d)|_{dB} = P_{Tx}|_{dBm} - \overline{P_{Rx}}|_{dBm}. \quad (1)$$

The calculated PL is showed in Fig. 3 shown with point. The d is the distance between Tx antennas and Rx antennas

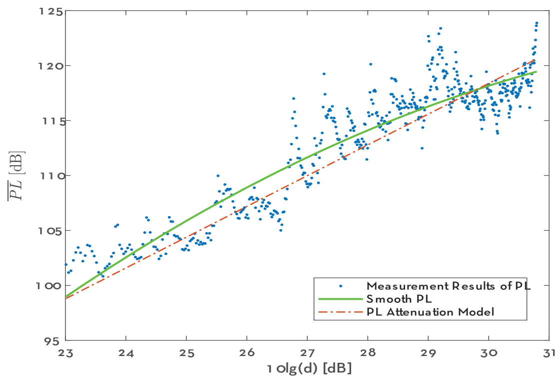

Fig. 3. Measured path loss and a path loss model with PL exponent 2.8.

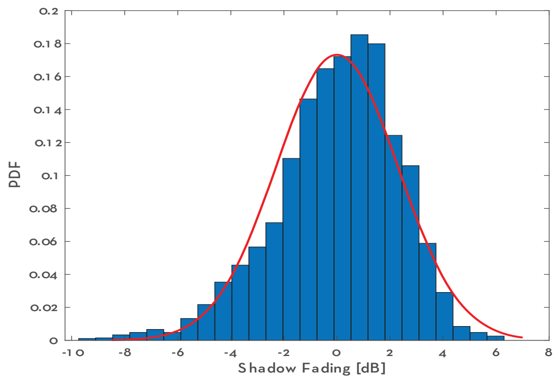

Fig. 4. Probability density function of large-scale fading.

(T-R). The calculated PL values are smoothed based on the least squares method and represented by a green line. Meanwhile, we fitted the measured PL to empirical PL model. The empirical average PL model is expressed as[7]

$$\begin{aligned}\overline{PL}(d)|_{dB} &= A + 10n_{att}\log_{10}(\frac{d}{d_0}) \\ &= A - 10n_{att}\log_{10}(d_0) + 10n_{att}\log_{10}(d) \\ &= \overline{PL}(d_0) + 10n_{att}\log_{10}(d),\end{aligned} \tag{2}$$

where $A = 20\log_{10}(\frac{4\pi d_0}{\lambda})$ is the free space path loss, λ is wavelength in the free space path loss expression, $\overline{PL}(d_0)$ represents the intercept value of the PL model at the reference distance of d_0 and n_{att} is the PL exponent. The n_{att} describes how quickly the wireless signal attenuates as a function of T-R distance. Considering the distance from the BS to the railroad and near-field effect, we choose the reference distance of d_0 = 200m to minimize the effects in large coverage cellular systems[8].

The measurement PL model at 465MHz is:

$$\overline{PL}(d)|_{dB} = 34 + 28\log_{10}(d). \tag{3}$$

The estimated PL exponent is about 2.8. The receiver antennas height in our measurement is approximately 4.05m. There are lots of scattered and reflected waves except the clear line-of-sight (LoS) in the wireless propagation path, which causes the n_{att} of the rural areas in HSR scene to be larger than the free space n_{att} value.

B. Large-Scale Fading

PL is not considered in the case of the same T-R distance. The surrounding environment in the same T-R distance with different locations is very different. For any d value, $PL(d)$ at a specific position is a random normal logarithmic distribution, which is given by

$$\begin{aligned}PL(d)|_{dB} &= \overline{PL}(d)|_{dB} + X_\sigma \\ &= \overline{PL}(d_0) + 10n_{att}\log_{10}(d) + X_\sigma,\end{aligned} \tag{4}$$

where X_σ denotes the shadow effect which is a zero-mean Gaussian distribution random variable and σ is the standard deviation. The units of X_σ and σ are dB. The formula (4) describes different random shadow fading at the same T-R distance. This phenomenon is known as log-normal shadowing. Shadowing is caused by obstacles between the transmitter and receiver. The shadow fading also is referenced as large-scale fading.

In order to calculate the large-scale fading of wireless channel, the received power is calculated by averaging the magnitude squared over 5 wavelengths so that the small-scale fading such as the multipath can be removed from the results and taking the sum over the delay domain. The choice of 5 wavelengths is due to the large-scale fading characteristics generally in the range of several wavelengths[9]. Therefore, one of the wireless subchannel average received power $\overline{P(it_{av})}$ can be given by[3]

$$\overline{P(it_{av},1)}|_{dB} = \frac{1}{L}\sum_{n=iL+1}^{(i+1)L}\sum_{k=1}^{K} 20\log_{10}|h(nt_{rep}, k\Delta\tau, 1)|, \tag{5}$$

where L is the number of snapshots, the snapshot repetition period t_{rep} is approximately $0.25ms$ and $\Delta\tau$ = $0.2\mu s$ denotes the delay resolution. In this paper, 5 wavelengths are equal to 3.2m. When the train speed is 340km/h, the average time window t_{av} is about $0.03s$, including L = 11 snapshots.

Then, remove PL from the $\overline{P(it_{av},1)}$ with least square where sliding windows are 11 snapshots. The Fig. 4 shows the probability density function (PDF) of the large-scale fading phenomenon of the wireless channel. We fitted the measurement large-scale fading to a Gaussian distribution, which is defined as

$$pdf(x) = \frac{1}{\sqrt{2\pi}\sigma}exp(-\frac{(x-\mu)^2}{2\sigma^2}), \tag{6}$$

where μ denotes average value of variable. The Gaussian distribution is indexed in red as shown in Fig. 4. Here, $\sigma = 2.50$dB, $\mu = -4.5 \times e^{-14}$. A standard deviation between the samples and the prediction can be a good measure of large-scale fading.

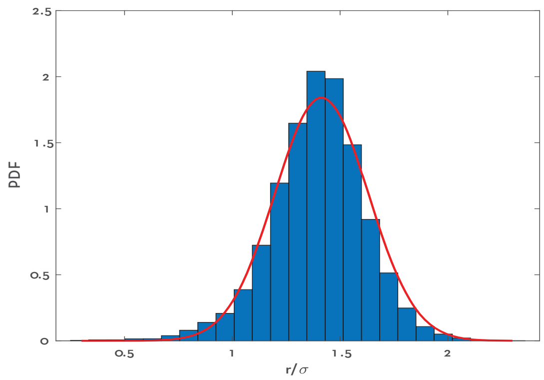

Fig. 5. Probability density function of small-scale fading.

C. Small-Scale Fading

1) Probability Density Function: In general, the received power fluctuates around an average value (local) over a very short distance. These fluctuations generally occur in about one wavelength. The phenomenon of the amplitude variation of the composite signal is small-scale fading caused by the mutual interference of different multipath components[9].

The PDF of small-scale fading is shown as Fig. 5. Here, r is the amplitude of each snapshot. At the same time, Rician distribution is fitted and marked as a red line. This is because there is the clear LoS path between T-R in the HSR scenario. The K-factor is a common characteristic parameter if the PDF of small-scale fading obeys the Rician distribution.

2) Two Moment-Based Estimations: The moments of the Rician distribution expressed by in terms of σ^2 and K-factor, are defined as[10]

$$\begin{aligned}\mu_n &= E[r^n(t_{rep})] \\ &= (2\sigma^2)^{\frac{n}{2}}\Gamma(\frac{n}{2}+1)exp(-K)_1F_1(\frac{n}{2}+1;1;K),\end{aligned} \tag{7}$$

where $r(t_{rep})$ is received signal envelop, which has a Rician distribution, σ^2 is variance of diffuse components, $\Gamma(\cdot)$ is the gamma function, and ${}_1F_1(\cdot;\cdot;\cdot)$ is the confluent hypergeometric function. We see from (7) that the moments determined by two parameters σ and K-factor. Hence, in order to get a moment-based K-factor, at least two different moments of $r(t_{rep})$ are needed. In the condition of $n \neq m$, the following function of K-factor is defined as

$$f_{n,m}(K) = \frac{\mu_n^m}{\mu_m^n}, \tag{8}$$

where μ_n is the nth moment of $r(t_{rep})$. From (8) we see that $f_{n,m}(K)$ depends only on K-factor. Therefore, an estimation of K-factor can be expressed as

$$\begin{aligned}\hat{K}_{n,m} &= f_{n,m}^{-1}(\frac{\mu_n^m}{\mu_m^n}), \\ \hat{\mu}_k &= \frac{1}{W}\sum_{l=0}^{W-1} r^k(lt_{rep}),\end{aligned} \tag{9}$$

where W is the number of snapshots. The moment estimator $\hat{\mu}_k$ can be updated using a sliding window of length W.

From (7) we can obtain that[11]:

$$\mu_1 = \frac{\sqrt{\pi}}{2}(\sigma^2)^{\frac{1}{2}}exp(-K)_1F_1(\frac{3}{2};1;K), \tag{10}$$

$$\mu_2 = s^2 + 2\sigma^2 = 2\sigma^2(K+1), \tag{11}$$

$$\mu_4 = 8\sigma^2 s^2 + 8\sigma^4 + s^4. \tag{12}$$

Substituting by (10,11,12) to (8), we obtain:

$$f_{1,2}(K) = \frac{\pi e^{-K}}{4(K+1)}[(K+1)I_0(\frac{K}{2}) + KI_1(\frac{K}{2})]^2, \tag{13}$$

$$f_{2,4}(K) = [\frac{(K+1)^2}{K^2+4K+2}]^2, \tag{14}$$

where $I_n(\cdot)$ is the nth-order modified Bessel function of the first kind. The $\hat{K}_{1,2}$ involves the complex numerical procedure of calculating the inverse function of (13). However, a simpler expression of $\hat{K}_{2,4}$ is obtained by (14) as following:

$$\hat{K}_{2,4} = \frac{-\hat{\mu}_2^2 + \hat{\mu}_4 - \hat{\mu}_2\sqrt{2\hat{\mu}_2^2 - \hat{\mu}_4}}{\hat{\mu}_2^2 - \hat{\mu}_4}. \tag{15}$$

Derived from the above, the $\hat{K}_{2,4}$ can be estimated directly by the moments of the received signal envelope. So $\hat{K}_{2,4}$ is used to estimate the K-factor in this paper.

3) The Result of K-factor: In order to get the characteristic of K-factor of small-scale fading, PL and large-scale fading components need to be removed first from measurement data to reduce their effects on the results. Local average power of the received signal is got by (5). Here, we use window size of 20 wavelengths[12], containing 41 snapshots. That is, K-factor is estimated every 12.9m along the railway. Then local average power can be removed from measurement data by

$$h_{norm}(nt_{rep}, k\Delta\tau, 1) = \frac{h(nt_{rep}, k\Delta\tau, 1)}{\sqrt{(P(it_{av}, 1))}}. \tag{16}$$

Here, the average time window t_{av} is about $0.14s$. At last, by estimating $\hat{\mu}_2$ and $\hat{\mu}_4$ according to (9), Rician parameters $\hat{K}_{2,4}$ can be computed by (15).

Cumulative distribution function (CDF) of K-factor is illustrated in Fig. 6 to evaluate the performance of the channel. It is seen from the trend of the CDF curve that the wireless propagation channel varies largely. The 90% values for CDF are from 2.22dB to 35dB. And the statistical properties, i.e, mean and standard variance (stv) are shown in TABLE II. The values of K-factor fluctuate within a large range with the mean value of 14.24dB, which means that there always exist a strong LoS path.

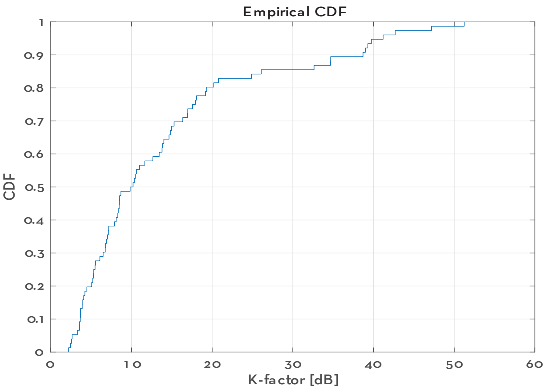

Fig. 6. Cumulative distribution function of K-factor.

TABLE II
STATISTICS OF THE K-FACTOR

Parameters	***Value***
Max (dB)	51.23
Min (dB)	2.22
Mean (dB)	14.24
Stv (dB)	12.1

IV. CONCLUSION

In this paper, PL, small-scale fading and large-scale fading model based on measurement data are especially investigated at the central frequency of 465MHz on HSR line. Measurement scenario and measurement system are introduced in detail. Here, typical rural area is mainly related. The USRP is mentioned for measuring LTE-R testing network. PL increases with distance in the form of logarithm. The PL exponent n_{att} is 2.8, which is the larger than the free space n_{att} value. Large-scale fading obeys Gaussian distribution with the $\sigma = 2.50$dB. Because of the strong LoS path of HSR scenario, small-scale fading is fitted to Rician distribution. The K-factor is estimated by using the moment-based estimated, which employs the second and the fourth moments of the signal envelope. The values of K-factor fluctuate dramatically according to the transceiver distance. And the mean K-factor based on analyzed data is about 14.24dB reflecting channel quality in HSR line. The measurement campaign and results are helpful in the broadband communication system design, modeling and optimization in HSR environment.

REFERENCES

[1] B. Ai, X. Cheng, and T. Kurner, and Z. D Zhong, “Challenges towards Wireless Communications for High Speed Railway,” IEEE Trans. Intell. Transp. Syst. vol. 15, no. 5, pp. 2143–2158, October 2014.
[2] P. Aiki, R. Gruber, and P. Vainikainen, “Wideband radio channel measurements for train tunnels,” IEEE Vehicular Technology Conference(VTC). Ottawa, pp: 460–464, 1998.
[3] L. Liu, C. Tao. and J. Qiu, “Position-based modeling for wireless channel on high-speed railwa under a viaduct at 2.35GHz,” IEEE J. Sel. Areas.Commun. vol. 30, no. 4, pp. 834–845, May 2012.
[4] R.S He, Z.D Zhong, B. Ai, and J. W Ding, “Propagation measurements and analysis for high-speed railway cutting scenario,” Electronics Letters, vol. 47, no. 21, pp. 1167–1168, October 2011.
[5] R.S He, Z.D Zhong, and B. Ai, “Path loss measurements and analysis for high-speed railway viaduct scene,” IEEE IWCMC. vol. 10, pp. 266–270, June 2010.
[6] J.H Wen, “Deep understanding of LTE-A,” Based on 3GPP RELEASE-11 protocol, unpublished.
[7] K. Sun, P. Wang, and Y.Z Li, “Path loss models for suburban scenario at 2.3 GHz, 2.6 GHz and 3.5 GHz,” IEEE. 2008.
[8] T. S. Rappaport, “Wireless communications: principles and practice,” 2nd ed. 2001, pp. 75–78.
[9] A. F. Molish, “Wireless Communications,” 2015.
[10] C. Tepedel, A. Abdi, and G. B, “The Ricean K factor: Estimation and performance analysis,” IEEE Transactions on Wireless Communication. vol. 2, no. 4, pp.834–845, July 2003.
[11] L. Gao, Z. Zhong, and B. Ai, “Estimation of the Ricean K factor in the high speed railway scenarios,” 5th Int Communications and Networking in China (CHINACOM) ICST Conf. pp. 1C-5, Aug 2010.
[12] W. C. Y. Lee, “Estimate of local average power of a mobile radio signal,” IEEE Trans. Veh. Technol. vol. VT-34, no. I, February 1985